water

MDPI

Article

Hydrogeochemistry and Strontium Isotopic Signatures of Mineral Waters from Furnas and Fogo Volcanoes (São Miguel, Azores)

Letícia Ferreira [1,*], José Virgílio Cruz [1,2], Fatima Viveiros [1,2], Nuno Durães [3], Rui Coutinho [1,2], César Andrade [1,4], José Francisco Santos [3] and Maria Helena Acciaioli [3]

1 IVAR—Instituto de Investigação em Vulcanologia e Avaliação de Riscos, Universidade dos Açores, 9500-321 Ponta Delgada, Portugal
2 FCT—Faculdade de Ciências e Tecnologia, Universidade dos Açores, 9500-321 Ponta Delgada, Portugal
3 GeoBioTec—Geobiociências, Geoengenharias e Geotecnologias, Departamento de Geociências, Universidade de Aveiro, 3810-193 Aveiro, Portugal
4 CIVISA—Centro de Informação e Vigilância Sismovulcânica dos Açores, Universidade dos Açores, 9500-321 Ponta Delgada, Portugal
* Correspondence: leticia.r.ferreira@azores.gov.pt

Abstract: This study focused on 13 water samples collected from two of the main active volcanoes (Furnas and Fogo) at São Miguel, Azores. Based on the major element composition, the waters are classified into Na-HCO_3 and Na-Cl types. While the concentrations of chloride seem to reflect the contribution of sea salt aerosols, the behavior of the main cationic species and Sr in the analyzed waters appear to have been largely controlled by the interaction between meteoric waters and the underlying bedrock. The temperature and input of CO_2 from the secondary volcanic activity are enhancing the silicate leaching. The stable isotopic data show that these waters have a meteoric origin ($\delta^{18}O$ = −2.03 to −4.29‰; $\delta^{2}H$ = −7.6 to −17.4‰) and are influenced by a deep hydrothermal/volcanic carbon source ($\delta^{13}C$ = −4.36 to −7.04‰). The values of $\delta^{34}S$ (0.13 to 12.76‰) reflects a juvenile sulfur source derived from the leaching of volcanic rocks. The Sr isotopic ratios show a slight difference between the values from Furnas ($^{87}Sr/^{86}Sr$ = 0.705235–0.705432) and Fogo ($^{87}Sr/^{86}Sr$ = 0.705509–0.707307) whereas the Furnas waters are less radiogenic. The Sr isotope also shows that the hydrochemical signatures of the groundwater was controlled by the rock leaching, and the samples Furnas reached water-rock isotopic equilibrium.

Keywords: $^{87}Sr/^{86}Sr$; mineral waters; water-rock interaction; hydrogeology of volcanic systems; Azores

Citation: Ferreira, L.; Cruz, J.V.; Viveiros, F.; Durães, N.; Coutinho, R.; Andrade, C.; Santos, J.F.; Acciaioli, M.H. Hydrogeochemistry and Strontium Isotopic Signatures of Mineral Waters from Furnas and Fogo Volcanoes (São Miguel, Azores). *Water* **2023**, *15*, 245. https://doi.org/10.3390/w15020245

Academic Editor: Guilin Han

Received: 15 November 2022
Revised: 15 December 2022
Accepted: 3 January 2023
Published: 5 January 2023

1. Introduction

Strontium (Sr) is a divalent alkaline earth element with an ionic radius (1.18 Å) similar to that of calcium (1.00 Å). This explains why Sr^{2+} can easily substitute Ca^{2+} in the crystal lattice of Ca-bearing minerals, such as plagioclase, apatite, titanite, calcite, aragonite, and dolomite [1]. Strontium has four naturally occurring isotopes, namely ^{84}Sr, ^{86}Sr, ^{87}Sr, and ^{88}Sr, whereas ^{87}Sr derives from the radioactive decay of the unique naturally occurring Rb isotopes, the ^{87}Rb through β-emission [1]. Rubidium is an alkali metal with an ionic radius (1.52 Å) sufficiently similar to the one of potassium (1.38 Å), which allows Rb^{+} to substitute K^{+} in K-bearing silicate minerals, such as K-feldspars, micas, and clay minerals [1].

The age and the Rb content of a rock are the major factors controlling the $^{87}Sr/^{86}Sr$ ratio [2,3]. The increase in isotope ratio is proportional to the Rb/Sr ratio, forming the basis of dating rocks using the isochron method. Hence older rocks, particularly those with high Rb/Sr ratios, tend to have larger variations between different minerals and higher $^{87}Sr/^{86}Sr$ ratios than younger rocks [4]. Consequently, old silicic crustal rocks with higher Rb/Sr ratios have the most radiogenic Sr isotopic signatures ($^{87}Sr/^{86}Sr > 0.709$). In contrast, young Rb-depleted basaltic rocks typically display the lowest $^{87}Sr/^{86}Sr$ ratios (0.703–0.706) [3].

Strontium isotopes are also an important tool in hydrogeology since $^{87}Sr/^{86}Sr$ ratios are very good hydrogeochemical tracers, as the high atomic weight of Sr prevents fractionation during natural processes [5]. Thus, the transference from the bedrock to circulating waters, soils, biosphere, and food webs occurs without appreciable modification of the $^{87}Sr/^{86}Sr$ ratios [4,6,7]. The $^{87}Sr/^{86}Sr$ ratios in groundwater depend on the Rb/Sr ratios and the age of the rocks with which they interact along their path [1]. Therefore, variations in the $^{87}Sr/^{86}Sr$ ratios can be ascribed to the mixing of Sr derived from different rock sources with distinct isotopic compositions [5]. In addition, as the kinetics of mineral dissolution reactions range over orders of magnitude, the Sr isotope ratios of solutes will be dominated by the most easily weathered minerals. For this reason, the $^{87}Sr/^{86}Sr$ is unlikely to be isotopically equilibrated with the whole rock [4]. In this context, the $^{87}Sr/^{86}Sr$ ratio in groundwater will therefore be a function of the weatherable Sr and the efficiency of its exchange [8].

Besides the rock-signature driver, other factors may influence Sr isotope ratios in aqueous systems, such as atmospheric inputs (rainfall), the residence time, and anthropogenic contamination (e.g., agricultural fertilizers). Thus, the use of Sr isotopes as tracers for study the origin and evolution of natural waters, or to characterize mixing processes with distinct isotopic signatures, requires a thorough knowledge of the rain $^{87}Sr/^{86}Sr$ ratio, geology and age of the rocky substrate, the chemical weathering reactions taking place in the region and the potential sources of anthropogenic contamination [4,6].

There are several case studies [4,5,9–11] that highlight the use of $^{87}Sr/^{86}Sr$ as tracers of weathering processes and flow pathways in surface water and groundwater in different landscapes. Strontium isotopes have been used to assess the origin of salinity in highly saline waters as well as a tracer of the origin of the water [4]. Ref. [12] verified that the higher $^{87}Sr/^{86}Sr$ ratio and lower Sr^{2+} concentrations in the groundwater of the Hongjiannao Lake Basin were derived from the dissolution of silicate minerals, whereas the opposite behavior was due to the dissolution of carbonate and sulfate minerals. They have also been used in active volcanic environments where, by combining major and trace elements and $^{87}Sr/^{86}Sr$, it was possible to characterize the processes that contribute to the mineralization of thermal waters [13].

In volcanic Azores archipelago numerous mineral water discharges are spread along the territory [14–17], namely in seven of the nine islands (São Miguel, Terceira, São Jorge, Pico, Faial, Graciosa, and Flores), presenting a wide range of dissolved solid content, hydrochemical characteristics, and temperature. Other secondary manifestations of volcanism also occur in the Azores archipelago, such as hydrothermal fumaroles and diffuse degassing areas [18–20]. The discharge of mineral waters in the main rivers that drains out the slopes of some central volcanoes, as Fogo and Furnas, both in São Miguel Island, also controls partially the composition of the river waters [21].

The compositional variations of the mineral water springs over the archipelago, especially at the São Miguel Island, have been characterized in several monitoring programs [14,15]. The stable isotopic composition has been used in several hydrogeological studies of mineral waters in the Azores, such as $\delta^{18}O$ and $\delta^{2}H$ ratios to confirm the meteoric origin of the waters [14,22], the $\delta^{13}C$ and $\delta^{34}S$ ratios to determine the volcanic origin of the dissolved gases [23], and the $\delta^{11}B$ ratio used for the characterization of hydrogeochemical processes and to constrain the volcanic influence over water composition [24].

Instead, radioactive isotopes, such as the Rb and Sr pair, has not been extensively used. Ref. [25] carried out a study on river erosion in São Miguel where they used $^{87}Sr/^{86}Sr$ isotopic ratios, which shows both the chemical weathering of the basaltic rocks and the contribution of atmospheric marine aerosols for the hydrochemical signatures of these surface waters. Strontium isotopes were also used in a study on groundwater salinization in Graciosa and Pico islands [26].

This study aims to characterize the behavior of Sr isotopic ratios in the mineral waters from Furnas and Fogo Volcanoes (São Miguel Island), providing a first approach of the

regional geochemical characteristics of the $^{87}Sr/^{86}Sr$ ratio in the mineral waters including cold-CO_2 rich waters to thermal discharges.

2. Geological Setting

The Azores archipelago is located in the North Atlantic Ocean, between 37° to 40° N latitude and 25° to 31° W longitude, at about 1500 km West of Portugal mainland (Figure S1). The archipelago is formed by nine volcanic islands, and the eruptive activity ranged from effusive eruptions, characterized by steady lava flows, to more explosive events, such as the caldera forming [27].

2.1. Overview of the Geology of São Miguel Island

São Miguel Island is dominated by three active trachytic central volcanoes with summit calderas (Sete Cidades, Fogo, and Furnas), linked by two active volcanic fissural zones (Picos and Congro Fissural Volcanic Systems) [27] (Figure S1—Supplementary Material online). The active central volcanoes are characterized by explosive trachytic volcanism, while basaltic effusive Hawaiian/Strombolian eruptions dominate in the fissural zones, with occasional trachytic eruptions [28].

Among the global ocean island lavas, rocks that erupted on São Miguel have been widely studied [27,29–31] and some geochemical characteristics have been highlighted [32]. Of the nine islands, São Miguel lavas are the most potassic and are among the most enriched in light rare earth elements (LREE) [27,32,33]. Ref. [30], confirmed a gradual enrichment in some incompatible elements from the West to the East of the island that were also observed in previous studies [32,34,35]. Ref. [36] revealed that the Northeast lavas are relatively more enriched in Cs, Rb, Th, U, and Pb, but more depleted in Sr, Ba, Ti, and, to a lesser extent, in Eu relative to the Sete Cidades lavas. This island exhibits 87Sr/86Sr ratios ranging between 0.703274 and 0.704673 [30], and it is possible to find a striking regional variation across the island, similar to the behavior of the trace elements. This suggests that different magma sources occur beneath São Miguel Island and that the high $^{87}Sr/^{86}Sr$ has become increasingly important in the center and the east of the island [29,30] (Figure S2—Supplementary Material online).

2.2. Fogo Volcano

Fogo Volcano started to be formed around 200 ka BP [37]. This volcano is truncated by a summit caldera with a diameter of 3.2 km and an area of 4.8 km^2, formed as a result of several collapse events, which floor is presently occupied by a lake [38]. Inside the caldera, it is possible to observe a pumice cone and several domes, whereas the flanks of the volcano are covered by thick pyroclastic deposits of trachytic nature (s.l.) [39]. Tectonic structures show a dominant NW–SE to NNW–SSE strike, defined by several alignments of domes, scoria and pumice cones, as well as by some linear segments of the drainage system [40].

Compositionally, the volcanism of the Fogo Volcano is bimodal, with a predominance of lithologies representative of trachitic magmas (fall pumice, pyroclastic flows, lava flows and domes), but also with significant presence of basaltic materials [41]. The volcanic rocks from Fogo range from basanite and alkaline basalts, that represent the least evolved rocks, through basaltic trachyandesite and trachyandesite, with intermediate compositions, to trachyte, representing the felsic extreme [41]. The less evolved rocks have olivine and clinopyroxene phenocrysts, and plagioclase is the most abundant in the matrix, with associated opaques (in always very significant proportions), clinopyroxene, olivine, and, in accessory amounts, apatite. Basaltic trachyandesite and trachyandesite have a relatively diverse phenocrysts composition, including clinopyroxene, anorthoclase, plagioclase, biotite, and olivine. The matrix contains plagioclase, alkaline feldspar, clinopyroxene, opaques, apatite, and biotite. At the felsic end, the matrix is essentially composed of alkaline feldspar and plagioclase, with minor amounts of aegirine-augite, biotite, apatite, amphibole brown, and opaque. Sanidine and anorthoclase are the most common phenocrystalline phases, but biotite, plagioclase, and olivine can also be found [41]. Strontium isotope data from

Fogo Volcano rocks are highly variable (0.703609–0.709234), and trachytic/syenitic rocks present higher $^{87}Sr/^{86}Sr$ than mafic rocks [41]. The heterogeneity of values is most likely caused by seawater-magma interaction in the magma chambers, as there is no evidence of mixing between magmas from different sources or contamination by foreign rocks based on geochemical data, nor that hydrothermal and/or meteoric alteration could be the cause of the dispersion of Sr isotopic values [41]. Ref. [42] also studied the isotopic variations within the Fogo A, a bulky plinian fall deposit [41], and observed a Sr isotopic variation in whole rocks (0.7049–0.7061), glass (0.7048–0.7052), and sanidine phenocrysts (0.7048–0.7062) [42].

The main hydrothermal manifestations of Fogo Volcano are located on the northern flank and seem to be associated with the NW–SE fault system that defines the so-called Ribeira Grande graben [18,43].

2.3. Furnas Volcano

Furnas is the eastern-most of the three active central volcanoes and its activity began about 100 ka BP [44,45]. Throughout most of its recent history, Furnas Volcano appears to have been an essentially explosive trachytic volcano with eruptions centered in the caldera, which is the result of several collapse events [40,44]. The main (outer) caldera is approximately 8 × 5 km in diameter, with its long axis oriented NE–SW. The inner caldera (6 × 3.5 km) also cuts the Povoação Caldera and the Furnas main caldera rim to the east [45]. The volcano is affected by fault systems trending WNW–ESE, NE–SW, north–south and NNW–SSE, expressed by volcanic alignments, linear valleys and caldera outlines [40].

Furnas stratigraphy is divided into three groups: the Upper (UFG), Middle (MFG), and Lower (LFG) Furnas groups [43]. The LFG and MFG comprise numerous trachytic pyroclastic units, with minor trachytic domes and basaltic cones [46]. The UFG is dominated by inter-bedded pumice lapilli and ash beds [44,47], and the mineral assemblages are broadly similar: alkali feldspar (anorthoclase-sanidine boundary), Fe-Ti oxides, biotite, clinopyroxene (diopside-augite boundary) and apatite. Some domes also contain sodalite and amphibole [33]. There is no information available about Sr isotopes in Furnas rocks. The only values we can use as a base are those from the Fogo A layer, which is also present in the Furnas stratigraphy.

Furnas also presents a large number of secondary manifestations of volcanism, such as fumaroles and steaming grounds [19], as well as numerous mineral waters discharges [15,16]. The degassing manifestations at Furnas volcanic system are located both inside the caldera and in the south flank of the volcano, at Ribeira Quente village. Similarly, to the observed at Fogo Volcano, the main degassing areas are also associated to NW-SE tectonic structures [19]. The influence of the degassing of deep-seated volatiles with a volcanic origin also influences the geochemistry of the lake that occupies the caldera floor [48].

3. Hydrogeological Setting

Groundwater is a strategic resource at the Azores, as about 98% of the water supply is supported by aquifers [49–51]. Two major aquifer systems occur in the archipelago [51–53]: (1) the basal aquifer system, which corresponds to freshwater lenses floating underlying saltwater, and (2) perched-water bodies. The basal aquifer system presents generally a very low hydraulic gradient, and groundwater extraction is made through drilled wells in the coastal area. Perched-water bodies correspond to pervious units at altitude confined by impermeable or very low permeability layers [50].

Mineral water discharges occur in seven of the nine islands (São Miguel, Terceira, São Jorge, Pico, Faial, Graciosa, and Flores) [15,21], and the dominant water types are Na-HCO_3 and Na-Cl, representing two main trends ("hydrothermal" and "marine"). The island of São Miguel is where the number and variety of discharges are higher [15]. Discharges are not equally spread on the island, which distribution shows an association with the three active central volcanoes, in particular, Furnas and Fogo Volcanoes [54].

According to the classification defined by [55], the climate in São Miguel can be considered as humid to super-humid, and mesothermal with dry summers using the

Köppen classification [56,57]. The average annual precipitation in this island is equal to 1722 mm/yr and the recharge rates range between 16% and 45% [58].

Groundwater resource estimates of São Miguel (3.7×10^8 m^3/yr) are above the Azores median value (median = 1×10^8 m^3/yr) [59]. Specific capacity at São Miguel ranges between 0.49 and 100 L/s m, with a median value of 1.1 L/s m [59]. Transmissivity ranging from 5.98×10^4 to 1.22×10^1 m^2/s, with a median value of 1.35×10^3 m^2/s, and about 45.4% of the estimates can be considered as intermediate values (1.16×10^4 to 1.16×10^3 m^2/s) [60].

4. Sampling and Analytical Techniques

A set of 13 mineral water springs were selected according to several criteria, as the total discharge and the diversity on the geological and hydrogeological environment, namely temperature and CO_2 content (thermal and cold CO_2-rich springs), belonging to groups 1 to 3, according to the classification provided by [14], and based on previous data sets from [15,17,21] (Figure 1a–c). All samples discharge from perched-water bodies.

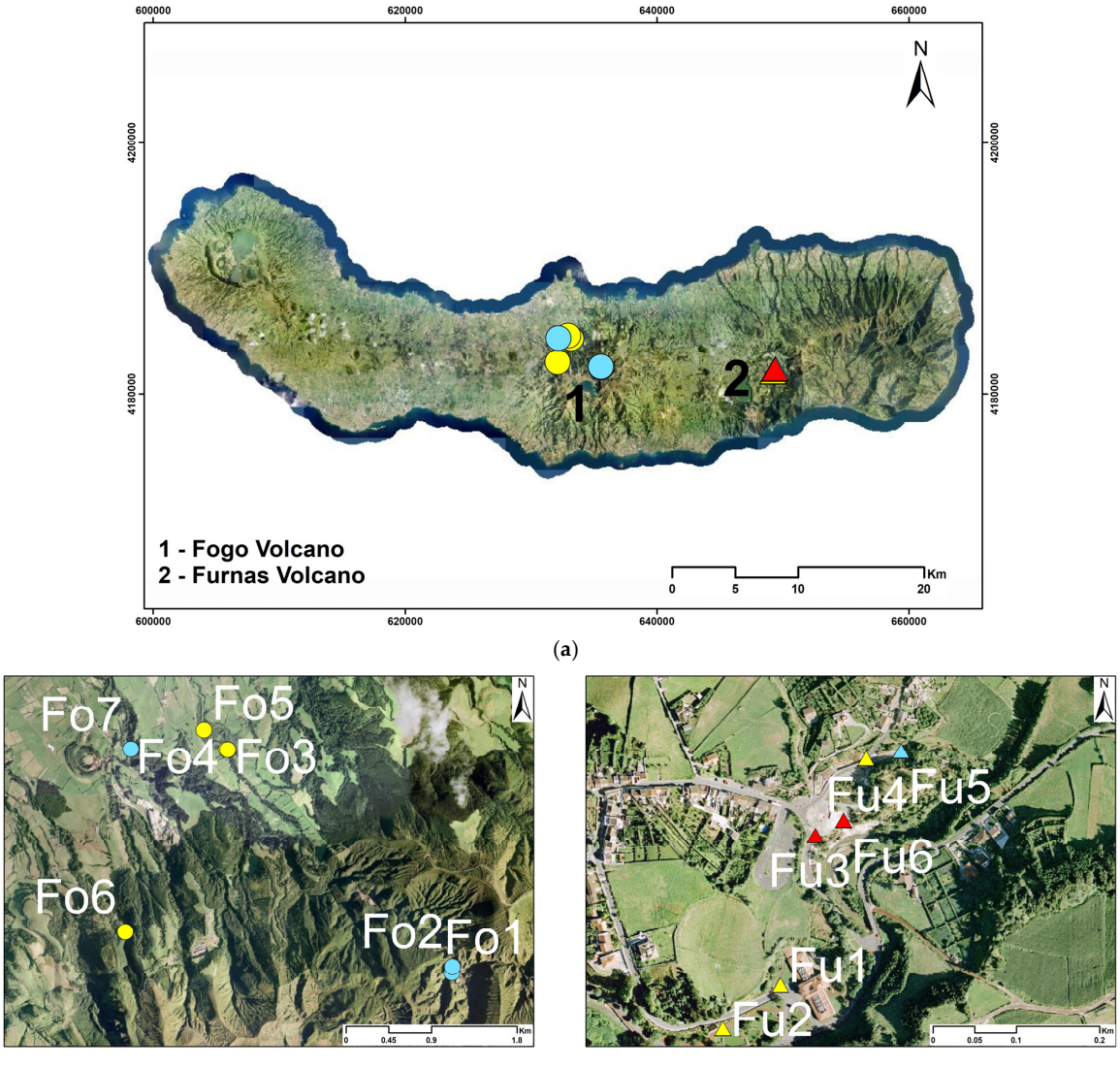

Figure 1. Location of the sampled waters along São Miguel Island (Azores). (**a**) map of São Miguel Island Showing the two volcanic units were the samples were collected; (**b**) samples collected in the northern flank of Fogo Volcano; and (**c**) samples collected inside the caldera complex of the Furnas Volcano.

Field measurements of temperature, pH, and electrical conductivity were made immediately after sampling using specific portable equipment (WTW pH/Cond 340i). Alkalinity and CO_2 titrations were made also in the field immediately after sampling, in both cases using well described routine methods [61]. Cation content (Na, K, Ca and Mg) was determined by atomic absorption spectrometry and the anionic composition (Cl and SO_4) by ion chromatography, in both cases using samples previously filtered (0.45 µm pore size cellulose membrane) in the field. Samples for atomic absorption analysis were acidified with suprapur® nitric acid immediately after being filtered. Silica was analyzed by spectrophotometry, using the silicomolybdic method. All the major-ion determinations were made in the hydrogeochemistry laboratory of the Research Institute for Volcanology and Risks Assessment (University of Azores).

Samples for the $\delta^{18}O$ and $\delta^{2}H$ (‰ vs. V-SMOW) determinations were collected in HDPE bottles following the standard procedure described by [62]. For the analysis of dissolved inorganic carbon (DIC) $\delta^{13}C$ (‰ vs. V-PDB) the sampling procedure proposed by the International Atomic Energy Agency [63] was followed. The analytical work was made at the Stable Isotope Laboratory of Estación Biológica Doñana—CSIC (Spain), using for the $\delta^{18}O$ and $\delta^{2}H$ determinations a Laser Spectrometer CRDS (Cavity Ring Down Spectroscopy) Picarro L2130-i, and a continuous flow isotope-ratio mass spectrometry system (Thermo Electron, Waltham, MA, USA), consisting of a Flash HT Plus elemental analyzer interfaced with a Delta V Advantage mass spectrometer, for $\delta^{13}C$. The analysis of the $\delta^{34}S$ were made in the Iso-Analytical laboratories through EA-IRMS (Isotope Ratio Mass Spectrometry), following standard sampling collection procedures.

Determination of the $^{87}Sr/^{86}Sr$ ratios was carried out in the ALS Environmental Laboratories (ALS Scandinavian, Luleå, Sweden) by MC-ICP-MS (NEPTUNE Plus, ThermoScientific, Waltham, MA, USA), using external calibration with bracketing isotope SRMs and after ion-exchange separation. The $^{87}Sr/^{86}Sr$ ratio of NIST SRM 987 (0.71034) was used for instrumental mass bias correction.

5. Results and Discussion

5.1. Hydrogeochemistry

The major ion composition, the physico-chemical parameters (temperature, pH, electrical conductivity) and SiO_2 content are shown in Table 1. The waters sampled can be divided into three types: boiling pools, thermal springs, and cold springs rich in CO_2.

The Caldeira Grande (Fu3) and the Caldeira Asmodeu (Fu6) are boiling pools (bpools), located in Furnas, which present temperatures values of 96.8 and 92.3 °C, respectively. The pH values are slightly neutral (7.96 and 7.91), and the electrical conductivity (EC) values vary between 2110 and 2370 µS cm^{-1}. The thermal waters (Fu1, Fu2, and Fu4; Fo3, Fo4, Fo5, and Fo6) discharge at temperatures between 29.3 and 75.6 °C with EC values varying from 166 to 1412 µS cm^{-1} and pH from 2.26 to 6.69, being in Fogo where thermal waters show higher acidity. The temperature and the EC of the cold springs rich in CO_2 (Fu5; Fo1, Fo2, and Fo7) varies from 16.6 to 18.8 °C and 292 to 564 µS cm^{-1}, respectively, and pH values close to 5.

Most of the waters from the Furnas area are of Na-HCO_3 type, excluding the Asmodeu sample (Fu6) classified as Na-Cl type (Figure 2). Fogo water samples are also classified as Na-HCO_3 (Fo1, Fo2, Fo3, and Fo4) and Na-Cl (Fo5, Fo6, and Fo7). The most important hydrogeochemical processes in volcanic aquifers is silicate hydrolysis, which releases alkali or alkali-earth metals, neutralizing water acidity and releasing HCO_3 in the system [64]. The HCO_3 enrichment originates from endogenous CO_2 in the soil and from fluid acidity neutralization through rock leaching, which is enhanced by water temperature [26].

Table 1. Physico-chemical parameters and chemical composition of water samples. (Type: Cold spr—cold spring; Thermal spr—thermal spring; bpool—boiling pools).

Location	Ref.	Name	Type	Altitude	T	pH	EC	CO_2	Na	K	Ca	Mg	Cl	SO_4	HCO_3	SiO_2	Sr	$^{87}Sr/^{86}Sr$	$\delta^{18}O$	$\delta^{2}H$	$\delta^{13}C$	$\delta^{34}S$
				m	°C		µS cm^{-1}	mg L^{-1}														
Furnas	Fu1	Quenturas	Thermal spr	199	57.6	6.67	1328	212.60	221.37	41.16	43.19	5.28	78.46	12.63	736.88	213.30	0.0638	0.705258	−3.73	−16.4	−7.04	11.1
	Fu2	Torno	Thermal spr	199	39.6	6.59	1412	234.00	264.19	28.01	54.73	7.28	93.01	10.28	608.78	148.81	0.0616	0.705235	−3.25	−13.3	−5.96	12.76
	Fu3	Caldeira Grande	bpool	203	96.8	7.96	2110	14.90	400.03	17.75	2.62	0.15	284.71	74.93	668.56	344.93	0.0224	0.705432	0.43	−0.9	−4.36	6.03
	Fu4	Caldeirão	Thermal spr	202	75.6	6.69	476	127.60	83.94	17.81	11.91	1.65	34.79	8.74	128.10	160.47	0.0217	0.705325	−3.73	−14.5	−4.54	1.77
	Fu5	Azeda	Cold spr	201	16.6	4.98	308	936.30	36.19	19.10	11.91	2.68	17.75	16.62	88.45	94.45	0.0228	0.705368	−4.04	−16.4	−5.76	3.28
	Fu6	Caldeira Asmodeu	bpool	199	92.3	7.91	2370	46.40	411.98	28.53	2.43	0.13	269.80	111.43	311.10	338.59	0.0187	0.705408	2.83	10.4	−3.00	−4.02
Fogo	Fo1	Lombadas	Cold spr	578	17.8	5.36	326	803.70	65.73	19.73	14.48	2.57	17.04	4.23	192.76	100.99	0.0252	0.706346	−4.29	−16.3	−5.4	4.85
	Fo2	Lombadas Furo II	Cold spr	578	18.6	5.69	564	881.00	60.57	37.00	22.13	3.88	18.46	4.71	184.22	103.39	0.0539	0.706495	−4.26	−16.4	−6.64	10.48
	Fo3	Cald. Pequena—CRG	Thermal spr	263	53.3	2.26	683	259.40	25.69	21.52	15.01	1.95	28.05	92.22	-	196.34	0.0272	0.705509	−2.03	−7.6	−6.82	0.73
	Fo4	Cald. Grande—CRG	Thermal spr	263	48.0	3.15	624	177.30	24.17	15.37	8.68	1.74	23.08	67.24	-	112.71	0.0095	0.706406	−2.17	−7.9	−5.7	0.13
	Fo5	Pocinha	Thermal spr	252	29.3	5.05	220	362.80	20.31	11.49	5.28	0.97	22.37	13.93	25.62	84.92	0.0060	0.706091	−4.06	−19	−6.46	0.87
	Fo6	Caldeira Velha Spr.	Themal spr	417	31.6	5.46	166	222.10	14.25	3.72	6.89	1.63	19.88	41.31	19.52	41.17	0.0047	0.707307	−4.27	−15.8	−7.18	6.63
	Fo7	Magarça	Cold spr	194	18.8	5.01	292	398.60	35.55	9.45	8.21	2.46	57.51	3.94	14.03	68.05	0.0229	0.706104	−4.1	−17.4	−5.9	11.36
—-	SW	Seawater	spr		-	-	-	-	-	-	-	-	-	-	-	-	7.8390	0.709199	0.49	5.9	−9.71	21.37

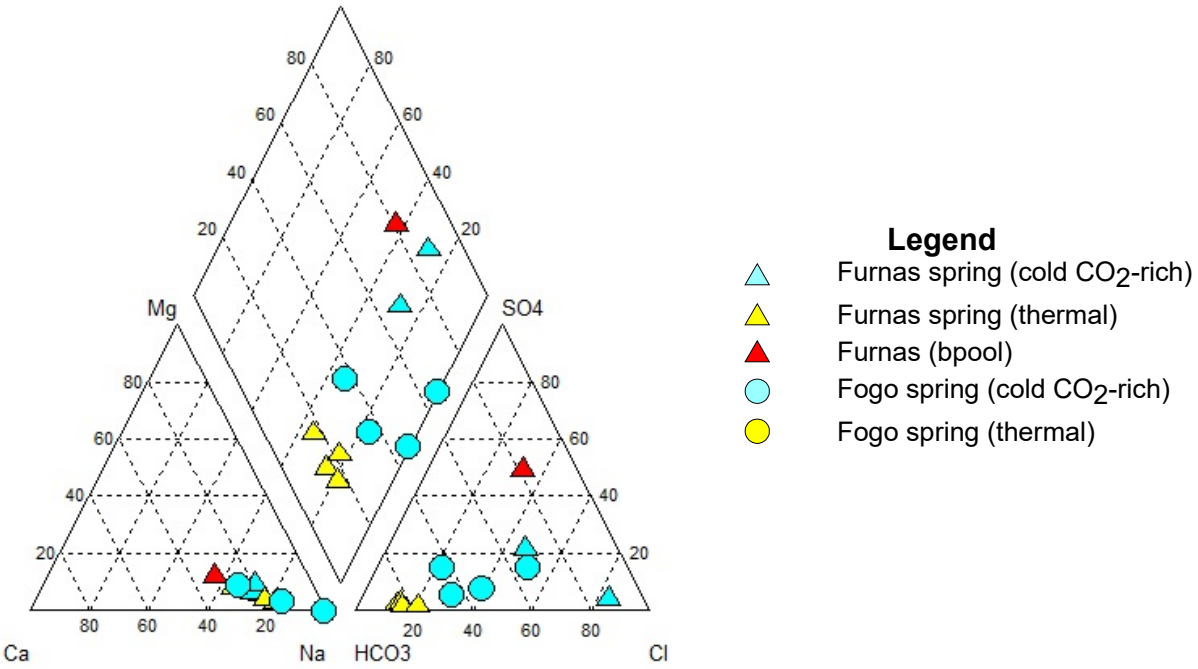

Figure 2. Relative major-ion composition of the sampled waters represented by a Piper-type diagram.

The Na and Cl content for the sampled waters were represented in a binary plot (Figure 3a). The chloride ion behaves as a conservative element in natural waters, as it does not interfere in most water-rock chemical rebalancing reactions, nor in soil leaching processes. Thus, the respective content is mainly controlled by physical factors (concentration/dilution), except in very specific geological environments (evaporites catchment) [65,66]. Chloride can originate from rain inputs (sea salt aerosols), human activities [10], and volcanic gases [67]. Since seawater spraying controls rainwater chemistry in coastal areas in general [68], and some samples are projected near the seawater dilution line, the Cl inputs can be ascribed to marine aerosols. This process influences the composition of groundwater discharges all over the archipelago as already suggested by [49]. Furthermore, the Caldeira Grande (Fu3) and Asmodeu (Fu6) show an increase in the concentration of Cl, and considering that they are boiling temperature fumaroles, the enrichment in Cl can be a result from evaporation processes.

Besides the contribution of a marine source, the plot of some samples above the seawater dilution line suggests the presence of another Na source (Figure 3a). The Na, Ca, and Mg cations are very mobile and tend to be easily released into the solution during hydrolysis reactions of silicates [69]. This Na-enrichment however demonstrates the contribution of the dissolution of minerals from the volcanic rocks in the chemistry of the waters, possibly of plagioclase, clinopyroxene and/or amphibole, which are the main phases of sodium in the rocks of the region. The leaching of local volcanic rocks and their minerals was expected to influence the chemistry of the mineral waters, and the presence of high CO_2 contents, that in some fraction is involved in water-rock interaction or weathering [64], and/or the high temperatures in some sites will drive the weathering of rocks. Nonetheless, the geology inputs are not observed in all samples. The cold springs are projected near the seawater dilution line, with just a slight increase in Na. Still, comparing the thermal waters, the ones from Furnas show an increase in Na, as the boiling pools. These data demonstrate a greater influence of chemical weathering on the composition of the waters of Furnas, which can also be corroborated by the higher concentration of ions such as Ca and Mg in the Furnas thermal waters and boiling pools (Table 1).

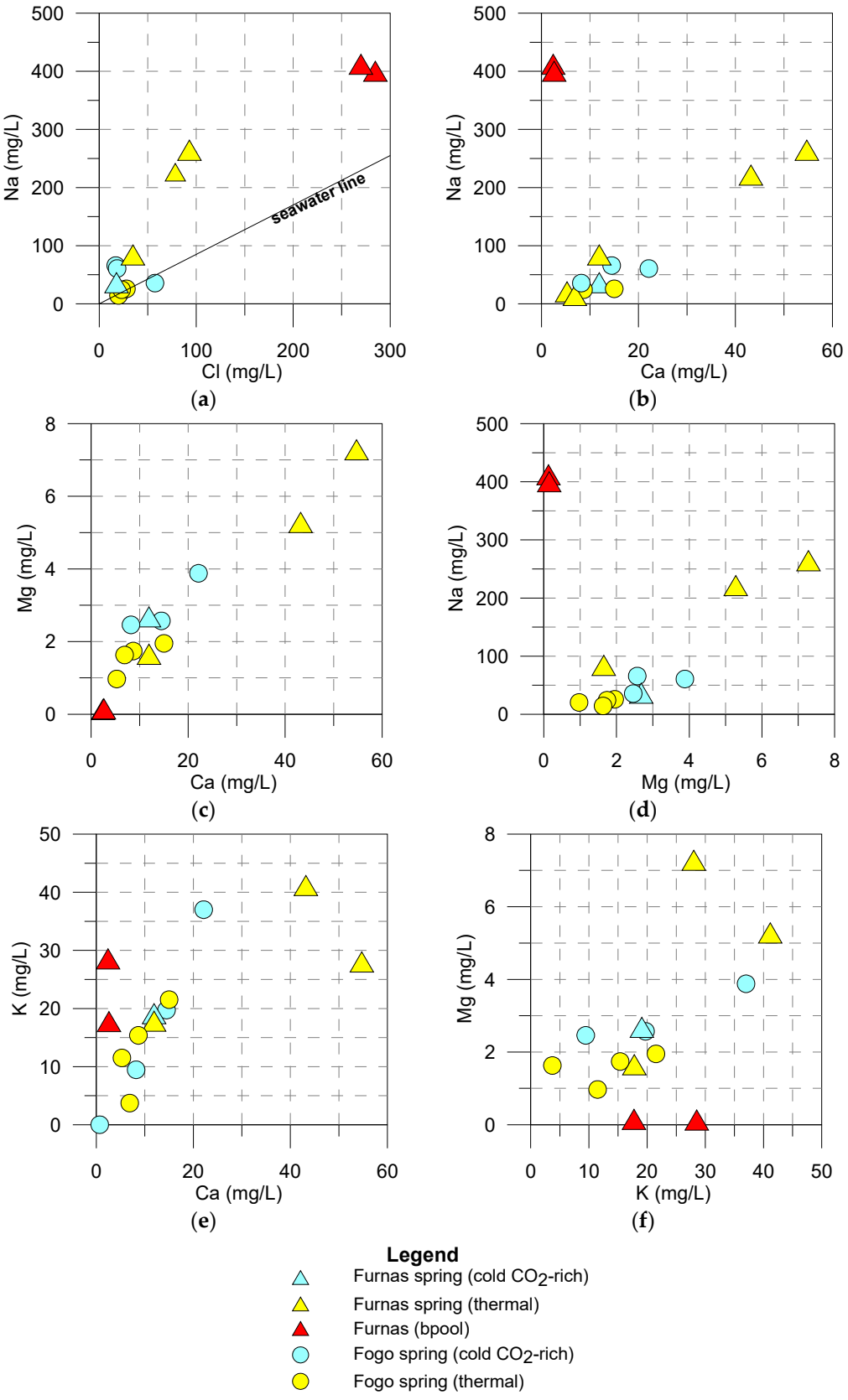

Figure 3. (**a**) Na vs. Cl bivariate plot (the seawater dilution line is shown); (**b**) Na vs. Ca bivariate plot; (**c**) Mg vs. Ca bivariate plot; (**d**) Na vs. Mg bivariate plot; (**e**) K vs. Ca bivariate plot; and (**f**) Mg vs. K bivariate plot of the mineral waters.

As shown in Figure 3b–d the main cations (Na, Ca, and Mg) demonstrate a positive correlation between them. This association suggests that their behavior must have been conditioned by the chemical weathering of clinopyroxene and/or amphibole, since Na, Ca, and Mg are incorporated in the crystalline structure of these minerals. As shown in [33], clinopyroxene is more abundant in the mineralogy of Furnas than amphibole, being most likely the mineralogical phase that most contributed to the chemistry of the mineral waters of Furnas. It is also noticeable, in all the samples, an influence of the dissolution of feldspars and biotite, which are supplying K to the solution. The positive correlation between K and Ca, as shown in Figure 3e, highlights the important role of the feldspars, particularly plagioclase, as a source of potassium and calcium in the waters. Although Alkali feldspar can also contribute with these elements to the solution, the role of plagioclase appears to be more prominent, as it has a higher weathering rate and reacts more easily. The contribution of plagioclase dissolution is more pronounced in Fogo waters (Figure 3e), which it's consistent with the site's geology. Potassium can also result from the chemical weathering of biotite, but it appears to play a minor role, as evidenced by the low correlation between Mg and K (Figure 3f).

The $\delta^{18}O$ and $\delta^{2}H$ content ranges, respectively, from −2.03‰ to −4.29‰ and −7.6‰ to −17.4‰, with the exception of Caldeira Grande boiling pool ($\delta^{18}O = 0.43$‰; $\delta^{2}H = -0.9$‰). Sampled waters $\delta^{18}O$ and $\delta^{2}H$ values are compared with the composition of the Global (GMWL) and Local Meteoric Water Line (LMWL). The LMWL corresponds to the isotopic composition of meteoric water in the period between 1962 and 2009 [70]. The lighter compositions are the ones presented by the cold springs and most of the discharges lie close to the local meteoric water line (LMWL) and the global meteoric water line (GMWL) (Figure 4), suggesting a meteoric origin as already discussed by [14]. The plot also shows a shift of the isotopic content from the boiling pools regarding the meteoric water lines, which suggests the influence of evaporation.

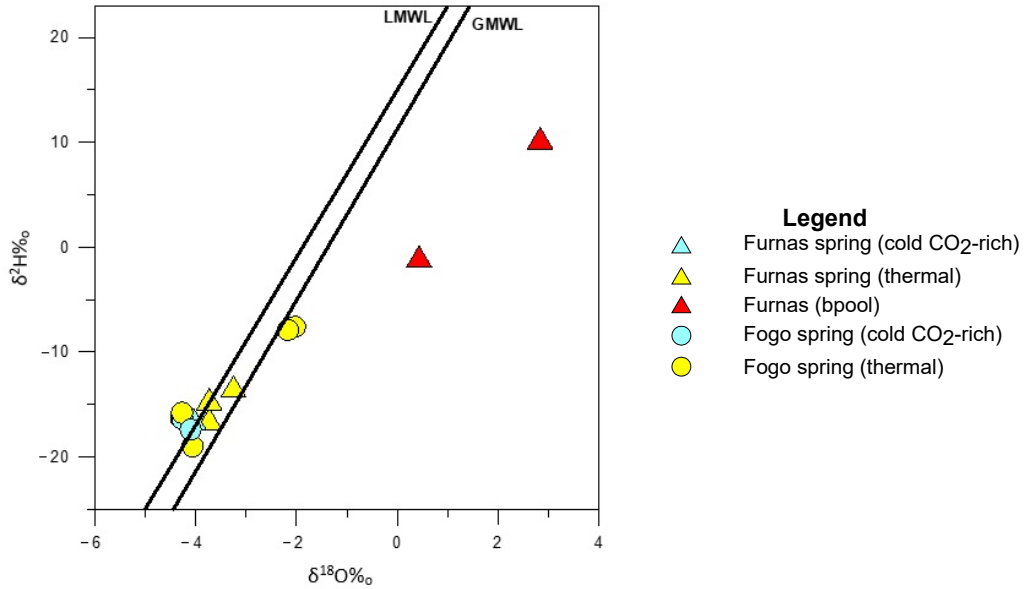

Figure 4. $\delta^{2}H$ vs. $\delta^{18}O$ bivariate plot of the sampled waters.

The $\delta^{13}C$ values are in the range between −4.36‰ and −7.04‰, closer to values presented by mantle CO_2 ($\delta^{13}C$ = −3.5‰ to −6‰) [71], thus presenting a heavier composition compared to modern atmosphere ($\delta^{13}C$ = −8.3‰) [72] and the much lighter $\delta^{13}C_{org}$ (~−20‰ to −33‰) [73]. The influence of carbon originated from a deep hydrothermal/volcanic source in Furnas emissions was preliminary suggested by [23] and [74]. Posteriorly, these observations have been confirmed through the $\delta^{13}C$ isotopic content of gas phases released in the boiling pools and in diffuse degassing areas [18,19]. The current study shows carbon isotopic compositions for the boiling pools in the same range of the

previous studies in the same areas [18], suggesting stability of these systems. Moreover, the $\delta^{13}C$ composition of Furnas Lake water also shows a much heavier value (−1.94‰) than biogenic values, suggesting the contribution of a deep carbon source, even if some fractionation processes may have interfered with the results [75].

The $\delta^{34}S$ in the sampled discharges range from 0.13‰ to 12.76‰, which are much lighter values compared to a marine source (21.37‰). The lighter $\delta^{34}S$ in the studied waters, with the exception of Caldeira de Asmodeu, are close to the isotopic content of gas phases in the boiling pools of Furnas (−2.1‰ to −0.7‰) [74], which reflects a juvenile sulfur source derived from volcanic gases. The heavier values result from mixtures of marine sulphur and the juvenile sulfur, as previously proposed by [74], as the latter should present values in the order of 0‰ to 5‰, which corresponds to the typical range of $\delta^{34}S$ in crystalline and volcanic rocks [76]. The value of $\delta^{34}S$ in Caldeira Asmodeu differs from the other samples. This water has the lowest value and is significantly lighter than the others. Such negative value suggest a contribution from oxidized isotopically light biogenic sulphide [1,22], which can be associated to the presence of stromatolitic structures observed in the thin sections of the precipitates [22].

5.2. Strontium Content and $^{87}Sr/^{86}Sr$

Strontium concentrations in the sampled mineral waters are extremely low, varying from 4.72×10^{-3} to 6.38×10^{-2} mg L^{-1} (Table 1). The sources of Sr in waters are several as atmospheric, dissolution of Sr-bearing minerals, and/or anthropogenic inputs [77]. In the water samples it is possible to notice a positive correlation with the ion pair Ca (Figure 5a), which can indicate a Sr contribution from the hosting rocks through which they flow. As previously stated, Sr can easily substitute Ca in the crystal lattice and, as perceived in the major ions hydrochemistry, these waters received an input of Ca from the host rocks which contain Ca-bearing minerals in their composition, such as clinopyroxene, amphibole and plagioclase. In addition to the Sr input from the geology, the Furnas thermal waters appear to be affected by some evaporation processes. According to [12], a positive relationship between the strontium and Cl concentrations, as shown by thermal waters from Furnas (Figure 5b), can indicate that evaporation has affected groundwater Sr concentrations.

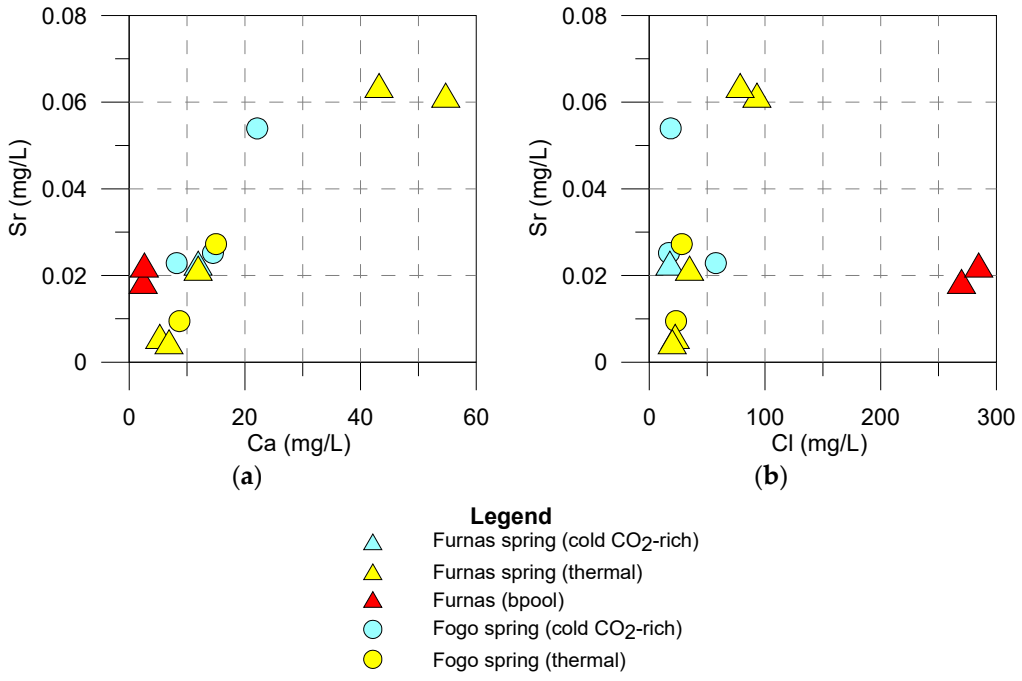

Figure 5. (**a**) Ca vs. Sr bivariate plot; and (**b**) Cl vs. Sr bivariate plot of the sampled waters.

The values of $^{87}Sr/^{86}Sr$ isotope ratios of the sampled waters are shown in Table 1 and their variability is illustrated in Figure 6. The Sr isotopic ratio obtained for seawater ($^{87}Sr/^{86}Sr$ = 0.709199) is within the standard value for the sea ($^{87}Sr/^{86}Sr$ = 0.70918 ± 1) [1], since the isotopic ratio for seawater is homogeneous at any given time [1,8].

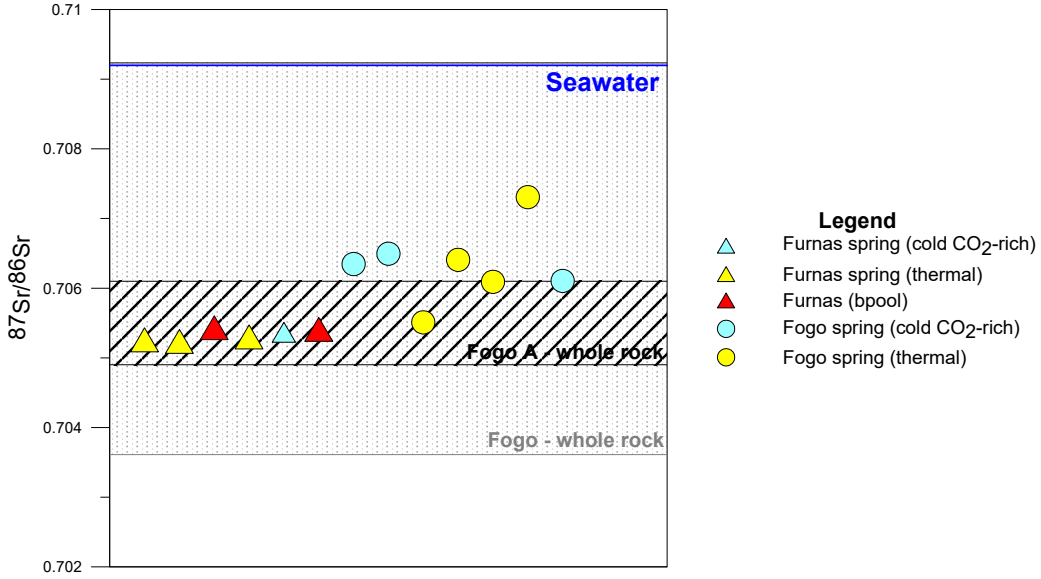

Figure 6. Display of the isotopic 87Sr/86Sr of the Furnas and Fogo samples. Whole-rock values for Fogo A were extracted from Snyder et al. (2004) [42] and Fogo whole-rock values were obtained from Santos et al. (2007) [41].

As shown in Table 1 and Figure 6, the mineral waters sampled exhibit a narrow range of $^{87}Sr/^{86}Sr$ ratios ($^{87}Sr/^{86}Sr$ = 0.705235–0.707307). Since these waters flow in relatively young volcanic rocks, that typically display the lowest $^{87}Sr/^{86}Sr$ ratios, it would be expected that the waters would depict low Sr isotopic values. Despite the low values and narrow range, it is possible to distinguish the waters from the two volcanoes, whereas the Furnas samples ($^{87}Sr/^{86}Sr$ = 0.705235–0.705432; Figure 6) are less radiogenic than the ones from Fogo ($^{87}Sr/^{86}Sr$ = 0.705509–0.707307; Figure 6). However, it is not possible to distinguish the different types of water (boiling pools, thermal and cold CO_2 rich) based on the $^{87}Sr/^{86}Sr$ ratios. The higher variability observed in the Fogo samples could be attributed to the samples' greater spatial distribution and the heterogeneous composition of the areas where the samples are collected. Instead, Furnas samples are all clustered together inside the caldera.

The results of the Sr isotopic data from the two volcanoes were compared to different intervals of $^{87}Sr/^{86}Sr$ whole-rock values. For the mineral waters from Fogo the values of Fogo Volcano whole rock values (0.703609–0.709234) [41] were used as reference (Figure 6), while the $^{87}Sr/^{86}Sr$ ratios of the Furnas waters were compared with the Fogo A whole rock values (0.7049–0.7061; Figure 6) [42] since this deposit is part of the Furnas stratigraphy and is the only deposit of this volcano with information about strontium isotopic content. Nevertheless, they display similar values to the $^{87}Sr/^{86}Sr$ whole-rock values (Figure 6), that is, these waters received a significant contribution from radiogenic Sr from the rocky matrix through which they circulate. The Furnas samples plot between the values of the limits for the Fogo A whole-rock, indicating that the water-rock isotopic equilibrium has been reached during the chemical weathering processes (Figures 6 and 7a). On the other hand, although the Fogo waters are also plot between the thresholds for the whole rock, the maximum limit of this range is similar to the values of seawater [41]. This fact associated with the influence of marine aerosols observed in the main hydrogeochemistry makes it difficult to know whether the waters circulating in these substrates have truly reached isotopic equilibrium, or if this results from the interaction of geology and marine aerosols.

If these values result from the mixing two different sources (i.e., host rocks and marine aerosols), the pattern in the $^{87}Sr/^{86}Sr$ vs. 1/Sr plot should be a straight line [4]. In the present case study, the behavior shown by the Fogo samples (Figure 7b) are too dispersed to consider a two-component mixing. This means that Fogo waters have reached the isotopic equilibrium or are the result from the mixing of three or more components. Taking into account the overall data, it seems that Fogo groundwater's isotopic ratios could have been heavily influenced by the chemical weathering processes, though it will be necessary to gather more data in order to determine the origin/origins of the isotopic Sr. This is based on the fact that Sr isotopic compositions of water in active volcano-hydrothermal systems closely match those of the reactant rocks. Other effects on the isotopic composition are negligible due to the highly accelerated fluid-rock interaction caused by the hot and highly acidic fluid dissolving in the volcanic gas [78]. If equilibrium was achieved, and given the wide range of $^{87}Sr/^{86}Sr$ values for Fogo rocks, the results presented by Fogo samples could indicate an origin in different aquifers or they could belong to the same aquifer but circulate in different layers, therefore presenting different paths.

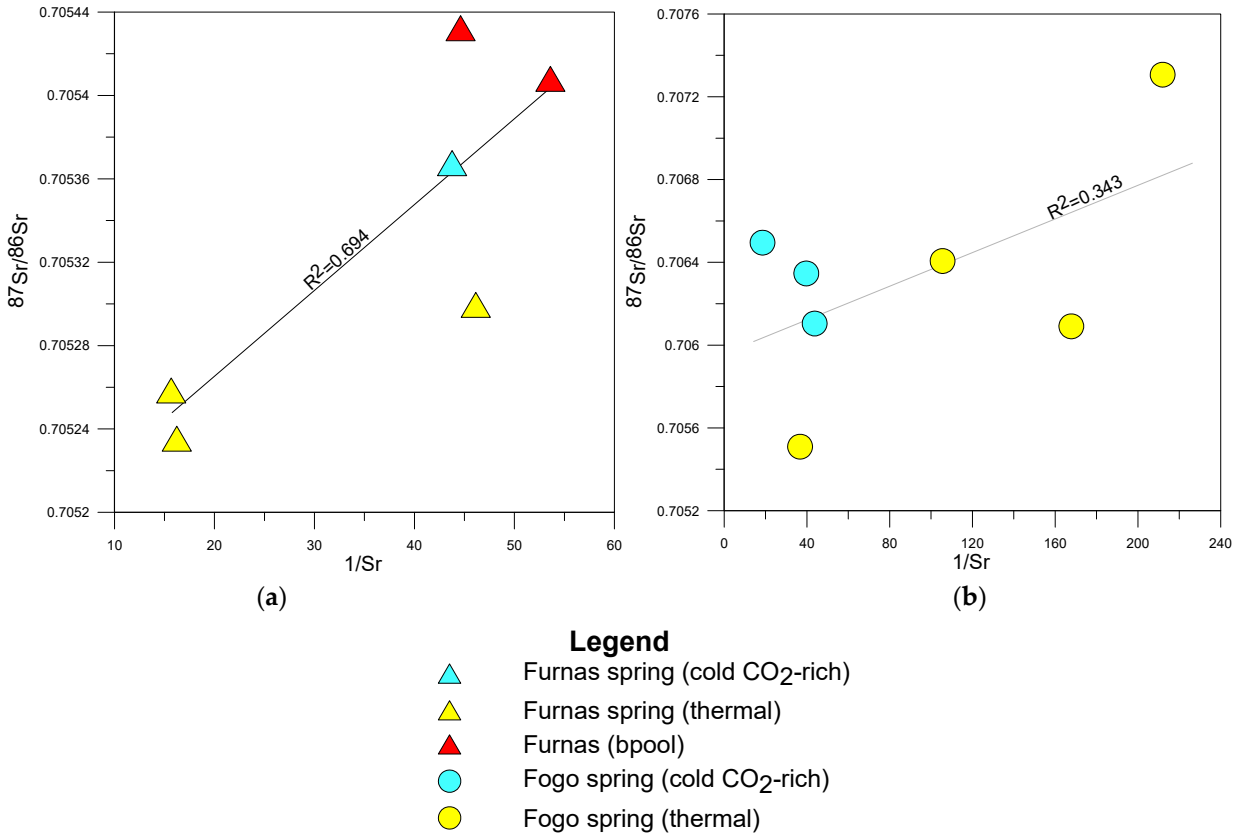

Figure 7. 1/Sr vs. $^{87}Sr/^{86}Sr$ content bivariate plot for: (**a**) Furnas; and (**b**) Fogo water samples.

Hence, the samples from both volcanos project within the range of values for the whole-rock used for comparison (Figure 6). Furnas reached the water-rock isotopic equilibrium during the chemical weathering processes. Given that the hydrothermal waters from São Miguel have a meteoric origin [14,22], which is noticeable in the main hydrogeochemistry, these groundwaters have lost the oceanic rain isotopic signature through the inputs of geology. Strontium isotopic ratios from Fogo suggests that the hydrochemistry of the groundwater was controlled by the rock leaching, nonetheless it is necessary more studies to conclude if the isotopic equilibrium was attained.

6. Conclusions

The origin of waters collected at the two hydrothermal active volcanic systems of Furnas and Fogo was characterized through their main hydrogeochemistry and Sr- isotopic compositions. Based on the major element composition, waters are classified into Na-HCO_3 and Na-Cl types. The behavior of the main cationic species and Sr isotopes reflects the interaction between meteoric waters (that transport marine aerosols) and the enclosing volcanic rocks (especially due to clinopyroxenes and amphiboles hydrolysis). It is possible to observe a higher contribution of the chemical weathering in the composition of the thermal waters from Furnas Volcano, promoted by the high temperature of the waters and, whereas the cold waters from both volcanos show similarities in the main ionic species. The stable isotopes (i.e., $\delta^{18}O$ and $\delta^{2}H$) ranges suggest a meteoric origin, as previously discussed. The $\delta^{13}C$ confirms the influence of carbon originated from deep hydrothermal/volcanic source, while $\delta^{34}S$ reflects a juvenile sulfur source derived from the volcanic gases.

In general, the isotopic $^{87}Sr/^{86}Sr$ ratios showed by the samples reveals that the mineral waters from Furnas are less radiogenic, allowing to distinguish these from the Fogo Volcano. However, it is not possible to notice an isotopic difference between the different types of water. The Sr isotopic ratios show that the mineral waters from Furnas reached water-rock equilibrium and it appears to indicate a similar hypothesis for Fogo.

This study gives us an insight into the geochemical characteristics of the $^{87}Sr/^{86}Sr$ ratio in the mineral waters of Furnas and Fogo (São Miguel), but further studies are required. For future work, the analysis of the rainwater (hydrochemistry and isotopic), the collection of more samples, as well as a more detailed analysis of the chemistry of the waters, mainly of minor ions (e.g., Rb), will be an opportunity to better understand the behavior and to identify the sources responsible for the Sr and $^{87}Sr/^{86}Sr$ signatures.

Supplementary Materials: The following supporting information can be downloaded at: https://www.mdpi.com/article/10.3390/w15020245/s1, Figure S1: Location of the Azores archipelago and São Miguel Island along the North-Atlantic Ocean; Figure S2: Map of São Miguel Island showing the major volcanic units according to Gaspar et al. (2015) [28] and the $^{87}Sr/^{86}Sr$ values (data from Beier et al., 2007 [30]).

Author Contributions: Conceptualization, L.F., J.V.C., and F.V.; methodology, J.V.C., C.A., and R.C.; software, L.F.; investigation, L.F., J.V.C., C.A., and F.V.; validation, L.F., J.V.C., F.V., N.D., C.A., R.C., J.F.S., M.H.A., and R.C.; writing—original draft preparation, L.F., J.V.C., F.V., and N.D.; writing—review and editing, L.F., J.V.C., F.V., N.D., C.A., R.C., J.F.S., and M.H.A.; visualization, L.F.; supervision, J.V.C., and F.V. All authors have read and agreed to the published version of the manuscript.

Funding: This study was funded by the project HEATSTORE—Geothermica Era net (European Project with Portuguese national funding from FRCT—Fundo Regional da Ciência e Tecnologia, Azores Government). Letícia Ferreira is supported by a PhD Grant from Fundação para a Ciência e Tecnologia (SFRH/UI/643/2020).

Conflicts of Interest: The authors declare no conflict of interest.

References

1. Faure, G.; Mensing, T.M. *Isotopes, Principles and Applications*, 3rd ed.; John Wiley & Sons: Hoboken, NJ, USA, 2005; p. 897.
2. Faure, G. *Principles of Isotope Geology*, 2nd ed.; John Wiley & Sons: New York, NY, USA, 1986.
3. Ribeiro, S.; Azevedo, M.R.; Santos, J.F.; Medina, J.; Costa, A. Sr isotopic signatures of Portuguese bottled mineral waters and their relationships with the geological setting. *Comun. Geol.* **2014**, *101*, 29–37.
4. Shand, P.; Darbyshire, D.P.F.; Love, A.J.; Edmunds, W.M. Sr isotopes in natural waters: Applications to source characterisation and water-rock interaction in contrasting landscapes. *Appl. Geochem.* **2009**, *24*, 574–586. [CrossRef]
5. Marques, J.M.; Carreira, P.M.; Goff, F.; Eggenkamp HG, M.; da Silva, M.A. Input of $^{87}Sr/^{86}Sr$ ratios and Sr geochemical signatures to update knowledge on thermal and mineral waters flow paths in fractured rocks (N-Portugal). *Appl. Geochem.* **2012**, *27*, 1471–1481. [CrossRef]
6. Capo, R.C.; Stewart, B.W.; Chadwick, O.A. Strontium isotopes as tracers of ecosystem processes: Theory and methods. *Geoderma* **1998**, *82*, 197–225. [CrossRef]

7. Frei, K.M.; Frei, R. The geographic distribution of strontium isotopes in Danish surface waters—A base for provenance studies in archaeology, hydrology and agriculture. *Appl. Geochem.* **2011**, *26*, 326–340. [CrossRef]
8. Åberg, G.; Jacks, G.; Hamilton, J. Weathering rates and $^{87}Sr/^{86}Sr$ ratios: An isotopic approach. *J. Hydrol.* **1989**, *109*, 65–78. [CrossRef]
9. Négrel, P.; Fouillac, C.; Brach, M. A strontium isotopic study of mineral and surface waters from the Cézallier (Massif Central, France): Implications for mixing processes in areas of disseminated emergences of mineral waters. *Chem. Geol.* **1997**, *135*, 89–101. [CrossRef]
10. Négrel, P.; Lemiere, B.; De Grammont, H.M.; Billaud, P.; Sengupta, B. Hydrogeochemical processes, mixing and isotope tracing in hard rock aquifers and surface waters from the Subarnarekha River Basin, (east Singhbhum District, Jharkhand State, India). *Hydrogeol. J.* **2007**, *15*, 1535–1552. [CrossRef]
11. Négrel, P.; Petelet-Giraud, E. Strontium isotopes as tracers of groundwater-induced floods: The Somme case study (France). *J. Hydrol.* **2005**, *305*, 99–119. [CrossRef]
12. Wu, C.; Wu, X.; Mu, W.; Zhu, G. Using isotopes (H, O, and Sr) and major ions to identify hydrogeochemical characteristics of groundwater in the Hongjiannao Lake Basin, Northwest China. *Water* **2020**, *12*, 1467. [CrossRef]
13. Bénard, B.; Famin, V.; Agrinier, P.; Aunay, B.; Lebeau, G.; Sanjuan, B.; Vimeux, F.; Bardoux, G.; Dezayes, C. Origin and fate of hydrothermal fluids at Piton des Neiges volcano (Réunion Island): A geochemical and isotopic (O, H, C, Sr, Li, Cl) study of thermal springs. *J. Volcanol. Geotherm. Res.* **2020**, *392*, 106682. [CrossRef]
14. Cruz, J.; França, Z. Hydrogeochemistry of thermal and mineral water springs of the Azores archipelago (Portugal). *J. Volcanol. Geotherm. Res.* **2006**, *151*, 382–398. [CrossRef]
15. Cruz, J.V.; Freire, P.; Costa, A. Mineral waters characterization in the Azores archipelago (Portugal). *J. Volcanol. Geotherm. Res.* **2010**, *190*, 353–364. [CrossRef]
16. Coutinho, R.; Fontiela, J.; Freire, P.; Cruz, J.V. Hydrogeology of São Miguel Island, Azores: A review. In *Volcanic Geology of São Miguel Island (Azores Archipelago)*; Gaspar, J.L., Guest, J.E., Duncan, A.M., Barriga, F.J.A.S., Chester, D.K., Eds.; Geological Society of London, Memoirs: London, UK, 2015; Volume 44, pp. 289–296.
17. Freire, P.; Andrade, C.; Viveiros, F.; Silva, C.; Coutinho, R.; Cruz, J.V. Mineral water occurrence and geochemistry in the Azores volcanic archipelago (Portugal): Insight from an extended database on water chemistry. *Environ. Earth Sci.* **2015**, *73*, 2749–2762. [CrossRef]
18. Caliro, S.; Viveiros, F.; Chiodini, G.; Ferreira, T. Gas geochemistry of hydrothermal fluids of the S. Miguel and Terceira Islands, Azores. *Geochim. Cosmochim. Acta* **2015**, *168*, 43–57. [CrossRef]
19. Viveiros, F.; Cardellini, C.; Ferreira, T.; Caliro, S.; Chiodini, G.; Silva, C. Soil CO_2 emissions at Furnas volcano, São Miguel Island, Azores archipelago: Volcano monitoring perspectives, geomorphologic studies, and land use planning application. *J. Geophys. Res. Solid Earth* **2010**, *115*, B12208. [CrossRef]
20. Viveiros, F.; Chiodini, G.; Cardellini, C.; Caliro, S.; Zanon, V.; Silva, C.; Rizzo, A.L.; Hipólito, A.; Moreno, L. Deep CO_2 emitted at Furnas do Enxofre geothermal area (Terceira Island, Azores archipelago). An approach for determining CO_2 sources and total emissions using carbon isotopic data. *J. Volcanol. Geotherm. Res.* **2020**, *401*, 106968. [CrossRef]
21. Freire, P.; Andrade, C.; Coutinho, R.; Cruz, J.V. Fluvial geochemistry in São Miguel Island (Azores, Portugal): Source and fluxes of inorganic solutes in an active volcanic environment. *Sci. Total Environ.* **2013**, *454*, 154–169. [CrossRef]
22. Woitischek, J.; Dietzel, M.; Inguaggiato, C.; Böttcher, M.E.; Leis, A.; Cruz, J.V.; Gehre, M. Characterization and origin of hydrothermal waters at São Miguel (Azores) inferred by chemical and isotopic composition. *J. Volcanol. Geotherm. Res.* **2017**, *346*, 104–117. [CrossRef]
23. Cruz, J.; Coutinho, R.M.; Carvalho, M.; Oskarsson, N.; Gislason, S.R. Chemistry of waters from Furnas volcano, São Miguel, Azores: Fluxes of volcanic carbon dioxide and leached material. *J. Volcanol. Geotherm. Res.* **1999**, *92*, 151–167. [CrossRef]
24. Morell, I.; Pulido-Bosch, A.; Daniele, L.; Cruz, J.V. Chemical and isotopic assessment in volcanic thermal waters: Cases of Ischia (Italy) and São Miguel (Azores, Portugal). *Hydrol. Process.* **2008**, *22*, 4386–4399. [CrossRef]
25. Louvat, P.; Allègre, C.J. Riverine erosion rates on São Miguel volcanic island, Azores archipelago. *Chem. Geol.* **1998**, *148*, 177–200. [CrossRef]
26. Cruz, J.V.; Andrade, C. Groundwater salinization in Graciosa and Pico islands (Azores archipelago, Portugal): Processes and impacts. *J. Hydrol. Reg. Stud.* **2017**, *12*, 69–87. [CrossRef]
27. Pacheco, J.M.; Ferreira, T.; Queiroz, G.; Wallenstein, N.; Coutinho, R.; Cruz, J.V.; Pimentel, A.; Silva, R.; Gaspar, J.L.; Goulart, C. Notas sobre a Geologia do Arquipélago dos Açores. In *Geologia de Portugal*; Dias, R., Araújo, A., Terrinha, P., Kullberg, J.C., Eds.; Escolar Editora: Lisboa, Portugal, 2013; Volume 2, pp. 595–690.
28. Gaspar, J.L.; Guest, J.E.; Duncan, A.; Chester, D.; Barriga, F. Volcanic Geology of São Miguel Island (Azores Archipelago): Introduction. In *Volcanic Geology of São Miguel Island (Azores Archipelago)*; Gaspar, J.L., Guest, J.E., Duncan, A.M., Barriga, F.J.A.S., Chester, D.K., Eds.; Geological Society of London, Memoirs: London, UK, 2015; Volume 44, pp. 1–3.
29. Hawkesworth, C.J.; Norry, M.J.; Roddick, J.C.; Vollmer, R. 143Nd/144Nd and 87Sr/86Sr ratios from the Azores and their significance in LIL-element enriched mantle. *Nature* **1979**, *280*, 28–31. [CrossRef]
30. Beier, C.; Stracke, A.; Haase, K.M. The peculiar geochemical signatures of São Miguel (Azores) lavas: Metasomatised or recycled mantle sources? *Earth Planet. Sci. Lett.* **2007**, *259*, 186–199. [CrossRef]

31. Zanon, V. Conditions for mafic magma storage beneath fissure zones at oceanic islands. The case of São Miguel Island (Azores archipelago). In *Chemical, Physical and Temporal Evolution of Magmatic Systems*; Geological Society of London: London, UK, 2015; Volume 422, pp. 85–104.
32. Widom, E.; Carlson, R.W.; Gill, J.B.; Schmincke, H.U. Th-Sr-Nb-Pb isotope and trace element evidence for the origin of the São Miguel, Azores, enriched mantle source. *Chem. Geol.* **1997**, *140*, 49–68. [CrossRef]
33. Jeffery, A.J.; Gertisser, R.; O'Driscoll, B.; Pacheco, J.M.; Whitley, S.; Pimentel, A.; Self, S. Temporal evolution of a post-caldera, mildly peralkaline magmatic system: Furnas volcano, São Miguel, Azores. *Contrib. Mineral. Petrol.* **2016**, *171*, 42. [CrossRef]
34. Elliott, T.; Blichert-Toft, J.; Heumann, A.; Koestsier, G.; Forjaz, V. The origin of enriched mantle beneath São Miguel, Azores. *Geochim. Cosmochim. Acta* **2007**, *71*, 219–240. [CrossRef]
35. Turner, S.; Hawkesworth, C.; Rogers, N.; King, P. U-Th isotope disequilibria and ocean island basalt generation in the Azores. *Chem. Geol.* **1997**, *139*, 145–164. [CrossRef]
36. Beier, C.; Haase, K.M.; Hansteen, T.H. Magma evolution of the Sete Cidades Volcano, São Miguel, Azores. *J. Petrol.* **2006**, *47*, 1375–1411. [CrossRef]
37. Muecke, G.K.; Ade-Hall, J.M.; Aumento, F.; MacDonald, A.; Reynolds, P.H.; Hyndman, R.D.; Quintino, J.; Opdyke, N.; Lowrie, W. Deep drilling in an activite geothermal area in the Azores. *Nature* **1974**, *252*, 281–285. [CrossRef]
38. Wallenstein, N.; Duncan, A.; Guest, J.E.; Almeida, M.H. Eruptive History of Fogo Volcano, São Miguel, Azores. In *Volcanic Geology of São Miguel Island (Azores Archipelago)*; Gaspar, J.L., Guest, J.E., Duncan, A.M., Barriga, F.J.A.S., Chester, D.K., Eds.; Geological Society of London, Memoirs: London, UK, 2015; Volume 44, pp. 105–123.
39. Wallenstein, N. Estudo da História Recente e do Comportamento Eruptivo do Vulcão do Fogo (S.; Miguel, Açores). Ph.D. Thesis, Universidade dos Açores, Ponta Delgada, Portugal, 1999; p. 266. (In Portuguese).
40. Carmo, R.; Madeira, J.; Ferreira, T.; Queiroz, G.; Hipólito, A. Volcano-Tectonic Structures of São Miguel Island, Azores. In *Volcanic Geology of São Miguel Island (Azores Archipelago)*; Gaspar, J.L., Guest, J.E., Duncan, A.M., Barriga, F.J.A.S., Chester, D.K., Eds.; Geological Society of London, Memoirs: London, UK, 2015; Volume 44, pp. 65–86.
41. Santos, J.F.; Acciaioli, M.H.; França, Z.; Nunes, J.C.; Pinto, M.S.; Forjaz, V.H. Contribuição para o estudo das Variações Lito-geoquímicas do Vulcão do Fogo (ilha de S.; Miguel, Açores). In Proceedings of theActas da XIV Semana de Geoquımica e do VIII Congresso de Geoquımica de Paıses de Lıngua Portuguesa, Aveiro, Universidade de Aveiro, Aveiro, Portugal, 11–16 July 2005; Volume 1, pp. 141–144.
42. Snyder, D.C.; Widom, E.; Pietruszka, A.J.; Carlson, R.W. The role of open-system processes in the development of silicic magma chambers: A chemical and isotopic investigation of the Fogo A trachyte deposit, São Miguel, Azores. *J. Petrol.* **2004**, *45*, 723–738. [CrossRef]
43. Pereira, M.L.; Matias, D.; Viveiros, F.; Moreno, L.; Silva, C.; Zanon, V.; Uchôa, J. The contribution of hydrothermal mineral alteration analysis and gas geothermometry for understanding high-temperatura geothermal fields. The case of Ribeira Grande geothermal field, Azores. *Geothermics* **2022**, *105*, 102519. [CrossRef]
44. Guest, J.E.; Gaspar, J.L.; Cole, P.D.; Queiroz, G.; Duncan, A.M.; Wallenstein, N.; Ferreira, T.; Pacheco, J.M. Volcanic geology of Furnas volcano, São Miguel, Azores. *J. Volcanol. Geotherm. Res.* **1999**, *92*, 1–29. [CrossRef]
45. Guest, J.E.; Pacheco, J.M.; Cole, P.D.; Duncan, A.M.; Wallenstein, N.; Queiroz, G.; Gaspar, J.L.; Ferreira, T. The volcanic History of Furnas Volcano, São Miguel, Azores. In *Volcanic Geology of São Miguel Island (Azores Archipelago)*; Gaspar, J.L., Guest, J.E., Duncan, A.M., Barriga, F.J.A.S., Chester, D.K., Eds.; Geological Society of London, Memoirs: London, UK, 2015; Volume 44, pp. 125–134.
46. Moore, R.B. Volcanic geology and eruption frequency, São Miguel, Azores. *Bull. Volcanol.* **1990**, *52*, 602–614. [CrossRef]
47. Cole, P.D.; Queiroz, G.; Wallenstein, N.; Gaspar, J.L.; Guest, J.E. An historic subplinianrphreatomagmatic eruption: The 1630 AD eruption of Furnas volcano, Azores. *J. Volcanol. Geotherm. Res.* **1995**, *69*, 117–135. [CrossRef]
48. Andrade, C.; Viveiros, F.; Cruz, J.V.; Coutinho, R.; Silva, C. Estimation of the CO_2 flux from Furnas volcanic Lake (São Miguel, Azores). *J. Geotherm. Res.* **2016**, *315*, 51–64. [CrossRef]
49. Cruz, J.V.; Amaral, C.S. Major ion chemistry of groundwater from perched-water bodies of the Azores (Portugal) volcanic archipelago. *Appl. Geochem.* **2004**, *19*, 445–459. [CrossRef]
50. Cruz, J.V.; Andrade, C. Natural background groundwater composition in the Azores archipelago (Portugal): A hydrogeochemical study and threshold value determination. *Sci. Total Environ.* **2015**, *520*, 127–135. [CrossRef]
51. Cruz, J.V.; Silva, M.O.; Dias, M.I.; Prudêncio, M.I. Groundwater composition and pollution due to agricultural pratices at Sete Cidades volcano (Azores, Portugal). *Appl. Geochem.* **2013**, *29*, 162–173. [CrossRef]
52. Cruz, J.V. Groundwater and volcanoes: Examples from the Azores archipelago. *Environ. Geol.* **2003**, *44*, 343–355. [CrossRef]
53. Cruz, J.V.; Silva, M.O. Hydrogeologic framework of the Pico Island (Azores, Portugal). *Hydrogeol. J.* **2001**, *9*, 177–189. [CrossRef]
54. Cruz, J.V.; Freire, P.; Costa, A.; Fontiela, J.; Cabral, L.; Coutinho, R.M. Hydrogeochemical Characterization of Mineral Waters in São Miguel Island, Azores. In *Volcanic Geology of São Miguel Island (Azores Archipelago)*; Gaspar, J.L., Guest, J.E., Duncan, A.M., Barriga, F.J.A.S., Chester, D.K., Eds.; Geological Society of London, Memoirs: London, UK, 2015; Volume 44, pp. 257–269.
55. Thornthwaite, C.W. An approach toward a national classification of climate. *Geogr. Rev.* **1948**, *38*, 55–94. [CrossRef]
56. Ricardo, R.P.; Madeira, M.A.V.; Medina, J.M.B.; Marques, M.M.; Sanches Furtado, A.F.A. Esboço pedológico da ilha de S. Miguel (Açores). *An. Inst. Super. Agron.* **1977**, *37*, 275–385.
57. Cruz, J.V.; Pacheco, D.; Cymbron, R.; Mendes, S. Monitoring of the groundwater chemical status in the Azores archipelago (Portugal) in the context of the EU water framework directive. *Sci. Total Environ.* **2010**, *61*, 173–186. [CrossRef]

58. DROTRH-INAG. *Plano Regional da Água-Relatório Técnico*; DROTRH-INAG: Ponta Delgada, Portugal, 2001. Available online: https://www.google.com/url?sa=t&rct=j&q=&esrc=s&source=web&cd=&cad=rja&uact=8&ved=2ahUKEwju9ZDKuK_8AhVGtVYBHflEDVkQFnoECBkQAQ&url=https%3A%2F%2Fservicos-sraa.azores.gov.pt%2Fgrastore%2FDRA%2FQSIGA%2FPP_DocumentoApoio.pdf&usg=AOvVaw22BHEM-kkz1K7wwgvAS4ci (accessed on 14 November 2022).
59. Cruz, J.V. *Ensaio Sobre a Água Subterrânea nos Açores. História, Ocorrência e Eualidade. SRA, Ponta Delgada*; 2004. Available online: https://www.google.com/url?sa=t&rct=j&q=&esrc=s&source=web&cd=&cad=rja&uact=8&ved=2ahUKEwjmn5Spt6_8AhU8s1YBHctVAlgQFnoECAgQAQ&url=http%3A%2F%2Fwww.ivar.azores.gov.pt%2Fpublicacoes%2FPaginas%2Fcms_908_CRUZ-J-V-2004-Ensaio-sobre-a-agua-subterranea-nos-Acores-Historia-ocorrencia-e-qualidade-Ed-Secretaria-Regional-do.aspx&usg=AOvVaw1zfHmlRlK5w206nxIKy1q4 (accessed on 14 November 2022).
60. Krásný, J. Classification of transmissivity magnitude and variation. *Ground Water* **1993**, *31*, 230–236. [CrossRef]
61. APHA-AWWA-WPCF. *Standard Methods for the Examination of Water and Wastewater*; American Public Health Association: Washington, DC, USA, 1985.
62. Clark, I.D.; Fritz, P. *Environmental Isotopes in Hydrology*; Lewis Publishers: New York, NY, USA, 1997; p. 328.
63. IAEA. *Sampling Procedures for Isotope Hydrology*; Water Resources Programe: Vienna, Austria, 2017.
64. Evans, W.; Sorey, M.; Cook, A.; Kennedy, B.; Shuster, D.; Colvard, E.; White, L.; Huebner, M. Tracing and quantifying magmatic carbon discharge in cold groundwaters: Lessons learned from Mammoth Mountain, USA. *J. Volcanol. Geotherm. Res.* **2002**, *114*, 291–312. [CrossRef]
65. Hem, J.D. *Study and Interpretation of the Chemical Characteristics of Natural Water*, 3rd ed.; Water-Supply Paper 2254; U.S. Geological Survey: Reston, VA, USA; p. 263.
66. Bestland, E.; George, A.; Green, G.; Olifent, V.; Mackay, D.; Whallen, M. Groundwater dependent pools in seasonal and permanent streams in the Clare Valley of South Australia. *J. Hydrol. Reg. Stud.* **2017**, *9*, 216–235. [CrossRef]
67. Kelly, W.R.; Panno, S.V.; Hackley, K.C. *The Sources, Distribution and Trends of Chloride in the Waters of Illinois*; Bulletin Illinois State Water Survey B-74; Illinois State Water Survey: Champaign, IL, USA, 2012; pp. 1–59.
68. Berner, E.K.; Berner, R.A. *Global Environment: Water, Air, and Geochemical Cycles*, 2nd ed.; Princeton University Press: Oxfordshire, UK; Princeton, NJ, USA, 2012; p. xvi + 444.
69. Custódio, E.; Llamas, M.R. *Hidrología Subterrânea*, 2nd ed.; Tomo, I., Ed.; Ediciónes Ómega, S.A.: Barcelona, Spain, 1983; p. 1157.
70. IAEA, Water Resource Programme. *Measurements of the Isotopic Composition of Meteoric Water of São Miguel, Azores from 1962 till 2009*; Water Resources Programe: Vienna, Austria, 2014.
71. Cartigny, P.; Harris, J.W.; Javoy, M. Diamond genesis, mantle fractionations and mantle nitrogen content: A study of δ^{13}C–N concentrations in diamonds. *Earth Planet. Sci. Lett.* **2001**, *185*, 85–98. [CrossRef]
72. Clark, T. *Groundwater Geochemistry and Isotopes*; CRC Press: Boca Raton, FL, USA; Taylor & Francis Group: London, UK, 2015.
73. O'Sullivan, P.E. Palaeolimnology. In *The Lakes Handbook, Limnology and Limnetic Ecology*; O'Sullivan, P.E., Reynolds, C.S., Eds.; Blackwell: Oxford, UK, 2004; Volume 1, pp. 609–666.
74. Ferreira, T.; Oskarsson, N. Chemistry and isotopic composition of fumarole discharges of Furnas caldera. *J. Volcanol. Geotherm. Res.* **1999**, *92*, 169–179. [CrossRef]
75. Andrade, C.; Viveiros, F.; Cruz, J.V.; Coutinho, R. Global carbon dioxide output of volcanic lakes in the Azores archipelago, Portugal. *J. Geochem. Explor.* **2021**, *229*, 106835. [CrossRef]
76. Kendall, C.; Doctor, D. Stable Isotopic Applications in Hydrological Studies. In *Surface and Groundwater, Weathering, and Soils*; Drever, J.I., Ed.; Elsevier: Amsterdam, The Netherlands, 2015; Volume 9, pp. 319–364.
77. Negrel, P.; Guerrot, C.; Millot, R. Chemical and strontium isotope characterization of rainwater in France: Influence of sources and hydrogeochemical implications. *Isot. Environ. Health Stud.* **2007**, *3*, 179–196. [CrossRef] [PubMed]
78. Ishikawa, H.; Ohba, T.; Fujimaki, H. Sr isotope diversity of hot spring and volcanic lake waters from Zao volcano, Japan. *J. Volcanol. Geotherm. Res.* **2007**, *166*, 7–16. [CrossRef]